EFFECT OF KINETIC PARAMETERS ON THE DYNAMICS OF CONTINUOUS CRYSTALLIZERS

Jaroslav NYVLT

Institute of Inorganic Chemistry, Academy of Sciences of the Czech Republic, 160 00 Prague 6, Czech Republic; e-mail: nyvlt@iic.cas.cz

Received March 6, 1997
Accepted November 4, 1997

Continuous crystallizers can exhibit periodic cycles of supersaturation, production rate, suspension concentration, crystal size and related quantities. These cycles are most pronounced at the beginning of the crystallization process and depend on the value of kinetic parameters whether they are damped during the run time. Apparently, the cycling behaviour of the crystallizing system depends on the value of ratio of the nucleation and growth exponents *n/g*. The higher the value of this ratio, the more pronounced is the instability of the system. Admixtures that have a significant effect on the kinetic parameters can dramatically affect the dynamic behaviour of crystallizers so that the steady state may not be established at all.

Key words: Crystallization; Crystallizer dynamics; Nucleation; Cycling behaviour; Crystal growth rate; MSMPR crystallizer.

It has been stated that periodic changes of supersaturation, solid phase content, crystal size and production rate of a continuous crystallizer can occur and extend over a considerable time[1–21]. The explanation of this phenomenon is as follows: First, the supersaturation rises and leads to the birth of a large number of nuclei. The surface area of these nuclei is low at the beginning of crystallization and increases slowly so that significant desupersaturation due to crystal growth starts with an appreciable time lag. The drop of the supersaturation results in a decrease in the growth rate of present crystals and in nucleation rate, so that due to a continuous withdrawal of the product, the number of crystals and their surface area decrease below their steady-state values. This, in turn, will cause an increase of the supersaturation and thus of the nucleation rate, and the result of such a sequence of events is then the occurrence of limit cycles. Evidently, the values of kinetic parameters of crystallization must affect the dynamic behaviour of the crystallizer and because they are strongly affected by certain admixtures[22], the presence of various impurities may accomplish the crystallization process even in such a way. The establishment of the steady state may be very slow in some cases, and the determination of kinetic parameters using a MSMPR (Mixed Suspension–Mixed Product Removal) crystallizer[23] may be sometimes almost impossible for this reason.

Some of the papers cited above show that the stability limit is given by the value of the nucleation exponent $n = 21$. This value is unusually high, however, and undamped cycling has been found even with much lower values[1]. In addition, the growth rate plays an important role here, too. The aim of this paper is to investigate the effect of kinetic parameters of nucleation and of growth on the dynamic behaviour of the continuous MSMPR crystallizer using the solution of corresponding differential equations by steps.

THEORETICAL

Let us consider a well-agitated crystallizer with a continuous feed of clear supersaturated solution and with continuous removal of suspension identical with that in the bulk (MSMPR crystallizer). The crystallizer contains a system consisting of such an amount of solution or suspension that contains 1 kg of free solvent, *i.e.*, the solvent that is not formally attached to the crystallizing substance. The unit time interval applied in the solution of the set of equations is 1 s.

The mathematical model is based on the calculation of the change in supersaturation given by the equation

$$(\Delta w_t - \Delta w_{t-1})/\Delta t = s - k_N \Delta w_{t-1}^n - k_G A_c \Delta w_{t-1}^g \qquad (1)$$

showing that the supersaturation change within the unit time interval is given by the supersaturation rate s and the decrease of supersaturation due to the nucleation and growth of crystals.

The number of crystals born during the unit time interval at time t is

$$N^*_{c(t)} = \frac{k_N \Delta w_t^n}{3\alpha\rho_c L_N^3} \Delta t \qquad (2)$$

with initial crystal size equal $L_{(t)} = L_N = L_0$. Crystals already present in the solution grow by the increment

$$\Delta L_t = \frac{k_G \beta}{3\alpha\rho_c} \Delta w_t^g \Delta t \qquad (3)$$

so that the size of crystals in the i-th fraction is $L_{i,t} = L_{i,t-1} + \Delta L_t$ with $L_0 = L_N$. Here $L_{i,t}$ denotes the size of crystals born at time i and grown until time t.

A part of crystals in any fraction is withdrawn as the product so that for the i-th fraction (for $i = 1$ to $i = t$),

$$N_{c,i} = N^*_{c,i} (1 - \Delta t / t_l) \tag{4}$$

holds, and the total number of crystals in a unit amount of suspension is then $N_{c,t} = \sum_{i=1}^{t} N_{c,i}$ The average crystal size is

$$L_{m,t} = \frac{\sum_{i=0}^{t} L_{i,t} N_{i,t}}{\sum_{i=0}^{t} N_{i,t}} \ . \tag{5}$$

Surface area of crystals needed for the calculation of crystal growth is

$$A_{c,t} = \beta N_{c,t} L^2_{m,t} \ , \tag{6}$$

and their mass is

$$m_{c,t} = \alpha \rho_c N_{c,t} L^3_{m,t} \ . \tag{7}$$

The specific production rate of the crystallizer is given by the equation

$$P_t = m_{c,t} / t_l \ . \tag{8}$$

The whole cycle represented by the equations given above is then repeated for the next time step: the time t is increased by 1 s and the new supersaturation, number of born crystals, crystal size increment, mean crystal size and their mass and surface area as well as the specific production rate are calculated using Eqs (*1*) to (*8*) again.

RESULTS AND DISCUSSION

Based on the equations shown in the theoretical part, a series of simulations has been performed using various kinetic parameters of crystallization, k_N, n, k_G and g, corresponding to kinetic equations for nucleation rate

$$B = k_N \Delta w^n \tag{9}$$

and that for crystal growth rate

$$G = k_G A_c \Delta w^g \quad . \tag{10}$$

Initial conditions correspond to the start with just saturated solution, *i.e.*, for $t = 0$, $\Delta w_0 = 0$, $N_c = 0$ holds. The standard set of parameters was arbitrarily chosen to be close to those of typical substances[24]

$$k_G = 0.02 \text{ kg}^{1-g} \text{ kg}_{fs}^{g} \text{ m}^{-2} \text{ s}^{-1}$$

$$g = 1$$

$$k_N = 0.01 \text{ kg}^{1-n} \text{ kg}_{fs}^{n-1} \text{ s}^{-1}$$

$$n = 3$$

$$L_N = 0.0001 \text{ m}$$

$$s = 3.33 \,.\, 10^{-4} \text{ kg kg}_{fs}^{-1} \text{ s}^{-1} \tag{11}$$

$$t_l = 600 \text{ s}$$

$$\alpha = 1$$

$$\beta = 6$$

$$\rho_c = 2\,000 \text{ kg m}^{-3} \quad .$$

Typical results of simultaneous using this set of constants are plotted in Fig. 1. As we could expect, the maxima of the Δw curve correspond to the minima of the L and the maxima of the N_c curves and *vice versa*.

In order to show the effect of the kinetic parameters on the dynamics of the MSMPR crystallizer, the kinetic constants have then been varied within the range of usual values[24]: k_N from 0.00001 to 100 $\text{kg}^{1-n}\ \text{kg}_{fs}^{n-1}\ \text{s}^{-1}$, n from 1 to 10, k_G from 0.0002 to 0.5 $\text{kg}^{1-g}\ \text{kg}_{fs}^{g}\ \text{m}^{-2}\ \text{s}^{-1}$ and g from 1 to 2 with remaining parameters corresponding to the standard set listed above.

The effect of the nucleation rate constant, k_N, on the supersaturation, Δw, is depicted in Fig. 2. It can be seen from this figure that, for intensive nucleation (high k_N values), the crystallizer run is almost stable, at least after elapse of 6 to 10 retention times of

solution (as the retention time t_l = 600 s, the steady state is established after elapse of 3 600–6 000 s). On decreasing the nucleation rate, the periodic cycling continues for very long times. Very similar effect can be seen in Fig. 3 with the time plots of the production rate P in dependence on the nucleation rate constants. It can be seen from Fig. 3 that there is no steady state established for a very long period for low nucleation rates so that no representative sample can be extracted for MSMPR evaluations in these cases.

The values of the nucleation exponent, n, have been changed from 1 up to 10. The low values correspond in most cases[24] to secondary nucleation; most frequent values are between 3 and 4 but a few substances posses high values of n close to 10. The results are depicted in Fig. 4. It is apparent from this figure that the higher values of n, the more pronounced is the cycling tendency of the system. With high values of the exponent n, the specific production rate P (and, of course, also the suspension density m_c) periodically drop close to zero (see Fig. 4, curves *7* and *8*).

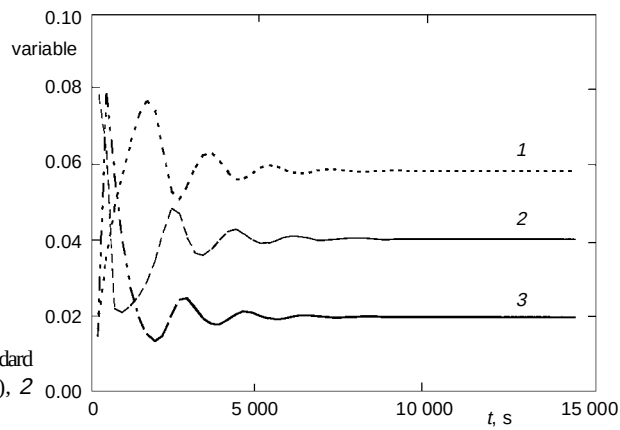

FIG. 1
Plot of results of simulation for the standard set of constants, Eqs (*11*): *1* $L \cdot 10^2$ (m), *2* Δw (kg kg_{fs}^{-1}), *3* $N_c \cdot 10^7$ (kg_{fs}^{-1})

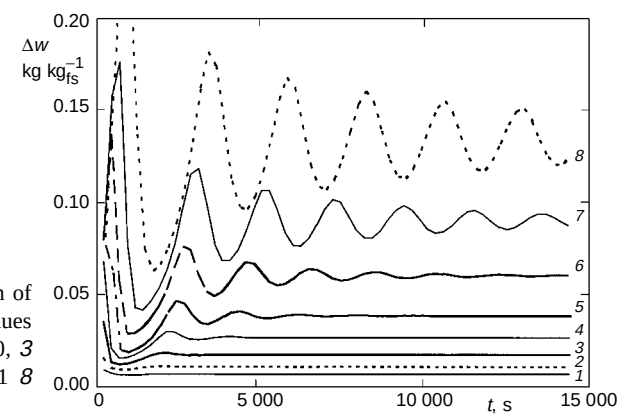

FIG. 2
Supersaturation plotted as a function of time for various nucleation rates (values of k_N) in $kg^{1-n}\,kg_{fs}^{n-1}\,s^{-1}$: *1* 100, *2* 10, *3* 1, *4* 0.1 *5* 0.01, *6* 0.001, *7* 0.0001 *8* 0.00001

The effect of the crystal growth rate G determined by the values of k_G and g is depicted in Figs 5 and 6. It can be seen from these figures that the decrease of the growth rate constant k_G increases the stability of the system but the sensitivity to this parameter is not very high. On the contrary, increase of the value of the growth rate exponent g significantly improves the tendency to quickly achieve the steady state. This latter effect seems to be opposite in comparison with the effect of the nucleation exponent n and, if we compare Fig. 7 (P–t plot for various values of n/g) with Fig. 4 (P–t plot for corresponding values of n), we can make out that similar ratios n/g exhibit

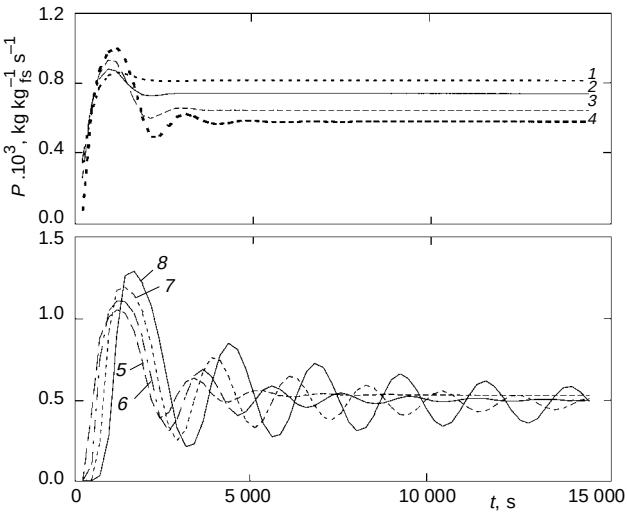

FIG. 3
Specific production rate, P, plotted as a function of time for various nucleation rates. Numbers of curves correspond to notation in Fig. 2

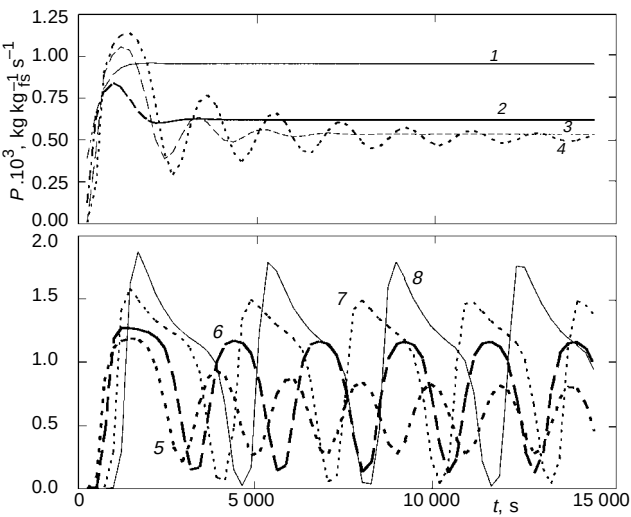

FIG. 4
Specific production rate P plotted as a function of time for various values of the nucleation exponent (n = 1 to 8) and standard set of remaining parameters. Numbers of curves correspond to the values of n

similar effect on the dynamics of the crystallizer: curve *1* in Fig. 7 shows a rapid steadying and so does curve *2* in Fig. 4; curves *2* and *3* in Fig. 7 exhibit a similar behaviour as curves *4* and *6* (or possibly 5) in Fig. 4, and curve *4* in Fig. 7 shows undamped oscillations like curves *6* to *8* in Fig. 4.

One of our preceding papers[25] dealt with the crystallization of potassium sulfate in the presence of dichromate ions as an admixture. Whereas the metastable zone width measurements and batch experiments could be done with admixture concentrations up to 2 or 2.5 mass %, the MSMPR experiments could be performed with admixture concentrations up to 1% only; at admixture concentration 2%, the susepnsion concentration varied dramatically as observed by naked eye, and the steady state could not be reached. Kinetic data for simulations of the system mentioned are summarised in Table I. The growth rate constant of pure K_2SO_4 was taken from the literature[24] and that for

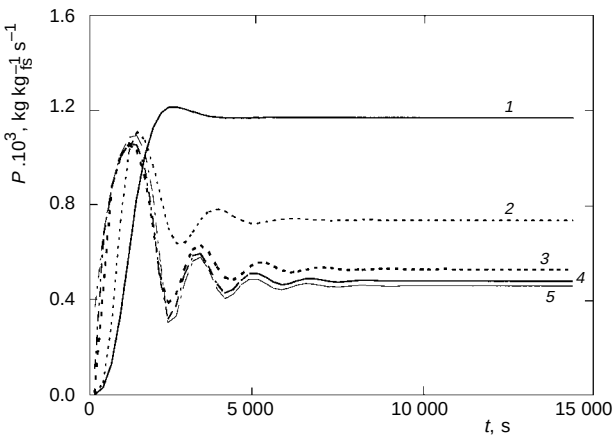

FIG. 5
The effect of the growth rate constant k_G (in $kg^{1-g}\ kg_{fs}^{g}\ m^{-2}\ s^{-1}$) on the dynamics of the system: *1* 0.5, *2* 0.1, *3* 0.02, *4* 0.002, *5* 0.0002

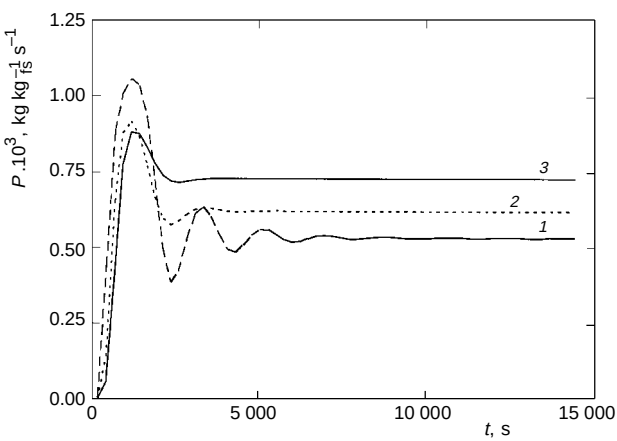

FIG. 6
The effect of the growth rate exponent g on the dynamics of the systems: g = *1* 1, *2* 1.5, *3* 2

TABLE I
Kinetic data of K_2SO_4 crystallization in the presence of $Cr_2O_7^{2-}$ ions

No.	$Cr_2O_7^{2-}$ wt.%	k_G $kg^{1-g}\,kg_{fs}^{g}\,m^{-2}\,s^{-1}$	g	k_N $kg^{1-n}\,kg_{fs}^{n-1}\,s^{-1}$	n
1	0	0.13	2	$1.26 . 10^{10}$	9.7
2	1	0.13	2	$2.08 . 10^{9}$	9.62
3	1	0.08	2	$2.08 . 10^{9}$	9.62
4	2	0.13	2	$8 . 10^{6}$	12.4

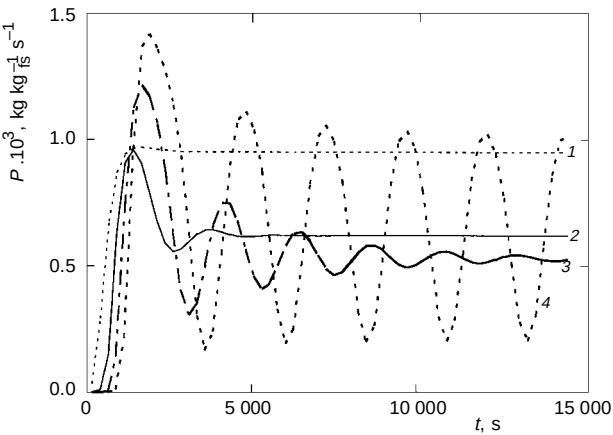

FIG. 7
Specific production rate P plotted as a function of time for values of the nucleation exponent n = 2 to 8 with g = 2, *i.e.*, n/g = 1, 2, 3 and 4. Numbers of curves correspond to values of n/g

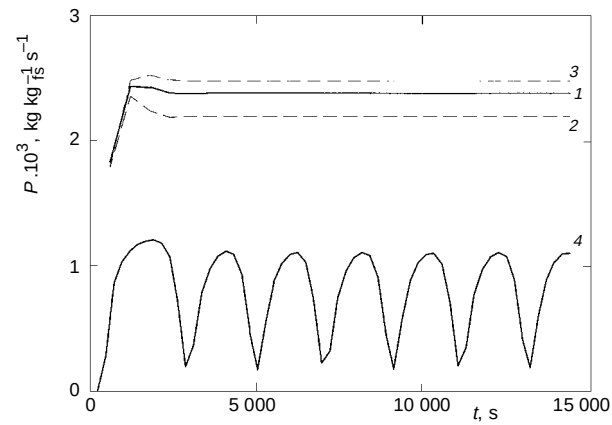

FIG. 8
Dynamic behaviour of continuous crystallization of K_2SO_4 without and with admixture of $Cr_2O_7^{2-}$ ions. Numbers of curves correspond to the notation in Table I

solutions with admixture recalculated using published growth rate data[25]. Nucleation constants were taken from the metastable zone width measurements[25].

Results of simulation runs are depicted in Fig. 8. It can be seen from this figure that the steady state with pure potassium sulfate as well as that with admixture concentration 1% is reached within the period of 6 times the retention time (t_l = 600 s and the dependences are stabilized after passage of 3 600 s), but the concentration of 2% of $Cr_2O_7^{2-}$ ions calls forth very intensive fluctuations so that steady state cannot be attained.

CONCLUSIONS

Continuous crystallizers can exhibit periodic cycles of supersaturation, production rate, suspension concentration, crystal size and related quantities. These cycles are most pronounced at the beginning of the crystallization and depend on the value of kinetic parameters whether they are damped during the run. The rise of the nucleation rate constant, k_N, has a stabilising effect and the same holds for low nucleation exponent, n. Decrease of the growth rate constant, k_G, increases the stability of the system, and the steadying effect rises with increasing the exponent of crystal growth, g. Apparently, the cycling behaviour of the crystallizing system depends on the value of the ratio of the nucleation and growth exponents n/g. The higher the value of this ratio, the more pronounced is the instability of the system.

Admixtures that have a significant effect on the kinetic parameters can dramatically affect the dynamic behaviour of continuous crystallizers so that the steady state may not be established.

SYMBOLS

(kg_{fs} denotes kg of free solvent, kg denotes kg of the solute.) The values are related to the volume containing 1 kg of free solvent, unit time interval Δt = 1 s.

A_c	surface area of crystals, $m^2\ kg_{fs}^{-1}$
B	nucleation rate, kg $kg_{fs}^{-1}\ s^{-1}$
G	crystal growth rate, kg $kg_{fs}^{-1}\ s^{-1}$
g	growth exponent
k_G	growth rate constant, $kg^{1-g}\ kg_{fs}^{g}\ m^{-2}\ s^{-1}$
k_N	nucleation rate constant, $kg^{1-n}\ kg_{fs}^{n-1}\ s^{-1}$
L	size of crystals, m
L_m	average crystal size, m
L_N	initial crystal size, m
ΔL	size increment, m
m_c	mass of crystals, kg kg_{fs}^{-1}
N_c	number of crystals, kg_{fs}^{-1}
$N_{c,t}^*$	total number of crystals at time t without product removal, kg_{fs}^{-1}
$N_{c,t}$	total number of crystals at time t after product removal, kg_{fs}^{-1}

$N_{c,(t)}$	number of crystals born during unit time interval at time t, kg$_{fs}^{-1}$
n	nucleation exponent
P	specific production rate of crystallizer, kg kg$_{fs}^{-1}$ s^{-1}
s	supersaturation rate, kg kg$_{fs}^{-1}$ s^{-1}
t	time, s
t_l	mean retention time of solution in the crystallizer, s
Δt	unit time interval (Δt = 1 s)
Δw	supersaturation, kg kg$_{fs}^{-1}$
α	volume shape factor
β	surface area shape factor
ρ_c	crystal density, kg m^{-3}
Subscripts	
c	solute, crystals
i	i-th interval, i-th fraction of crystals born in time $t = i$
m	average value
t	at time t
(t)	born at time t

This study has been supported by the Grant Agency of the Czech Republic, grant No. 2031045.

REFERENCES

1. Nyvlt J., Mullin J. W.: *Chem. Eng. Sci.* **1970**, *25*, 131.
2. Sherwin M. B., Shinnar R., Katz S.: *AIChE J.* **1967**, *13*, 141.
3. Sherwin M. B., Shinnar R., Katz S.: *Chem. Eng. Prog.* **1969**, *95* (*65*), 59, 75.
4. de Leer B. G. M., Koning A., de Jong E. J. in: *Industrial Crystallization* (J. W. Mullin, Ed.), p. 391. Plenum Press, New York 1975.
5. Todes O. M., Lugchenko A. K.: *Krist. Tech.* **1978**, *13*, 773.
6. Liss B., Shinnar R.: *AIChE Symp. Ser.* **1976**, *72* (*153*), 28.
7. Randolph A. D., Beckmann J. R., Kraljevich Z. I.: *AIChE J.* **1977**, *23*, 500.
8. Berliner L. V., Gorin V. N.: *Theor. Found. Chem. Eng.* **1976**, *10*, 337.
9. Nyvlt J.: *Collect. Czech. Chem. Commun.* **1978**, *43*, 2531.
10. Daudey P. J., de Jong E. J.: *J. Process Technol. Proc. 2, Ind. Cryst.* **1984**, 447.
11. Rohani S.: *Can. J. Chem. Eng.* **1986**, *64*, 112.
12. Akoghu K., Tavare N. S., Garside J.: *Chem. Eng. Commun.* **1984**, *29*, 353.
13. Lakatos B. G., Sapundzhiev T. J.: *Hung. J. Ind. Chem.* **1993**, *21*, 271.
14. Lakatos B. G.: *Comput. Chem. Eng.* **1994**, *18*, S427.
15. Lakatos B. G., Blickle T.: *Comput. Chem. Eng.* **1995**, *19*, S501.
16. Kramer H. J. M., de Woilf S., Jager J.: *ACS Symp. Ser.* **1990**, *438*, 159.
17. Suprinov N. A., Labutin A. N.: *Izv. Vyssh. Uchebn. Zaved., Khim. Khim. Tekhnol.* **1989**, *32*, 114.
18. Kind M., Nieken U.: *Chem. Eng. Process.* **1995**, *34*, 323.
19. Wojcik J. A., Jones A. G.: *Trans. Inst. Chem. Eng., A* **1997**, *75*, 113.
20. Leu Lii Ping: *Univ. Microfilms Int.*, **1982**, No. 8127742; *Chem. Abstr.* **1982**, *96*, 070957.
21. Tavare N. S.: *Industrial Crystallization – Process Simulation, Analysis and Design.* Plenum Publ., New York 1995.
22. Nyvlt J., Ulrich J.: *Admixtures in Crystallization*. Verlag Chemie, Weinheim 1995.

23. Randolph A. D., Larson M. A.: *Theory of Particulate Processes*. Academic Press, New York 1971.
24. Nyvlt J. Sohnel O., Matuchova M., Broul M.: *Kinetics of Industrial Crystallization*. Elsevier, Amsterdam and Academia, Prague 1985.
25. Nyvlt J., Zacek S.: *Cryst. Res. Technol*. **1996**, *31*, 763.